

Potential of Fluorescence Imaging Techniques To Monitor Mutagenic PAH Uptake by Microalga

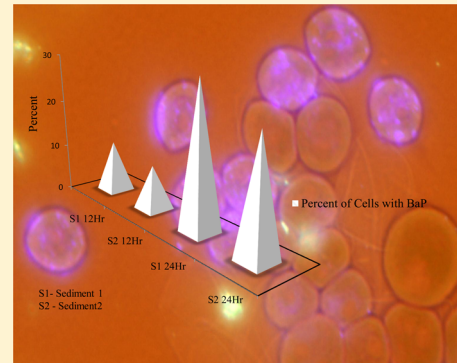
Suresh Ramraj Subashchandrabose,[†] Kannan Krishnan,^{*,†} Enrico Gratton,[‡] Mallavarapu Megharaj,[†] and Ravi Naidu[†]

[†]Centre for Environmental Risk Assessment and Remediation, University of South Australia and CRC CARE, Mawson Lakes, Adelaide, South Australia 5095, Australia

[‡]Laboratory for Fluorescence Dynamics, Department of Biomedical Engineering, University of California, Irvine, California 92697, United States

Supporting Information

ABSTRACT: Benzo[*a*]pyrene (BaP), a polycyclic aromatic hydrocarbon (PAH), is one of the major environmental pollutants that causes mutagenesis and cancer. BaP has been shown to accumulate in phytoplankton and zooplankton. We have studied the localization and aggregation of BaP in *Chlorella* sp., a microalga that is one of the primary producers in the food chain, using fluorescence confocal microscopy and fluorescence lifetime imaging microscopy with the phasor approach to characterize the location and the aggregation of BaP in the cell. Our results show that BaP accumulates in the lipid bodies of *Chlorella* sp. and that there is Förster resonance energy transfer between BaP and photosystems of *Chlorella* sp., indicating the close proximity of the two molecular systems. The lifetime of BaP fluorescence was measured to be 14 ns in *N,N*-dimethylformamide, an average of 7 ns in Bold's basal medium, and 8 ns in *Chlorella* cells. Number and brightness analysis suggests that BaP does not aggregate inside *Chlorella* sp. (average brightness = 5.330), while it aggregates in the supernatant. In *Chlorella* grown in sediments spiked with BaP, in 12 h the BaP uptake could be visualized using fluorescence microscopy.



INTRODUCTION

Benzo[*a*]pyrene (BaP), an extensively researched carcinogen and mutagen, belongs to the high-molecular-weight polycyclic aromatic hydrocarbon (PAH) group of chemicals. BaP and other PAHs are derived as a result of incomplete combustion and are released into the environment by both natural and anthropogenic activities. Some of the proven emission routes are domestic emission and wastes, automobile exhaust, industrial emission, agricultural activities, and also some natural sources.¹ Metabolism of BaP activates several mixed-function enzymes² in the cell and results in the progression of different types of cancer in human and animals. Being hydrophobic, BaP has been found to accumulate in several organisms, including microalgae,³ mussels,⁴ and mice.⁵

Microalgae are the primary producers in the food chain and can grow in three diverse ecosystems: fresh water, marine environments, and soil. They support many different life forms that are exclusively dependent on them for food and play a vital role in the environment.⁶ Microalgae growing in these environments are exposed to different pollutants, which may have natural or anthropogenic sources. Accumulation of pollutants by microalgae has an immediate effect on the higher organisms in the food chain that feed on them.⁷ The use of microalgae for the removal of different organic pollutants is also gaining importance,⁸ apart from their use as pollution

indicators.⁹ Studies related to the catabolic ability of microalgae to remove BaP were started recently. It has been shown that the green alga metabolizes BaP primarily to *cis*-dihydrodiols¹⁰ by a dioxygenase enzyme system similar to that in bacteria¹¹ and also forms BaP sulfate ester and glucose conjugates.¹² Most mammals and terrestrial plants follow the monooxygenase enzymatic pathway to metabolize BaP.¹²

Most of the biological effects exerted by BaP are mediated through aryl hydrocarbon receptors on the cell membrane.¹³ In mammalian cells, BaP is enzymatically converted into BaP-diol epoxide, which can complex with nucleotides to form nucleotide–BaP adducts.^{14,15} When these adducts are incorporated into DNA during DNA synthesis, the DNA polymerase is prevented from moving further as a result of interference by the adduct,¹⁶ which results in immature termination of DNA synthesis. Thus, defective metabolism or defective regulation of cellular metabolism occurs, which leads to apoptosis or proliferation of cells.¹⁷

Localization of BaP in murine macrophages and human fibroblasts has been demonstrated using fluorescence micro-

Received: January 23, 2014

Revised: July 14, 2014

Accepted: July 14, 2014

Published: July 14, 2014



copy.¹⁸ Fluorescence imaging of the BaP distribution in embryonic and larval medaka tissues has also been shown.¹⁹ It is essential to study the uptake and accumulation mechanisms of BaP in microalgae, as they are one of the primary producers in the food chain. Even though there have been previous reports showing accumulation of BaP³ in this system, intracellular localization and aggregation have not yet been studied using the most recent fluorescence microscopy tools. Determination of the bioaccumulation of organic compounds using standard analytical techniques such as GC and HPLC is invasive, as it requires killing of the organisms used for the study and the use of solvents to extract the organics. Fluorescence microscopy is a noninvasive technique that does not require harmful solvents for the extraction of organics. It also provides information about the accumulation pattern of hydrophobic pollutants inside single cells. Indeed, further studies are needed to develop quantitative microscopy tools to quantify the uptake of BaP and other fluorescent pollutants by microalgal cells. A microalgal cell contains a wide spectrum of autofluorescent molecules, and thus, it is difficult to distinguish fluorescence from additional molecules such as BaP accumulating in the cell unless a specific fluorescence signal that can be unequivocally attributed to BaP can be found. In an endeavor to study the accumulation of BaP and to visualize the intracellular localization, we used fluorescence lifetime imaging microscopy (FLIM) with the phasor approach and confocal microscopy with number and brightness (N&B) analysis.

The use of fluorescence microscopy and FLIM in algal studies was started recently,^{20,21} and these techniques have also been used extensively to study biological structures such as photosynthetic structures of plants.²² One advantage of FLIM is that the lifetime information can be represented as a phasor plot, thereby allowing better separation of fluorescent components and the identification of a specific lifetime signal from BaP. As the background fluorescence of plant cells has a very short lifetime, any fluorescent molecule that is different from the background can be well-separated in the phasor plot. The difference used could be either wavelength, which can be separated by filters, or lifetime, which can be resolved by a phasor plot. Hence, we used FLIM as the technique to detect and image the interaction of the fluorescent pollutant BaP with the microalga, *Chlorella* sp. We show that FLIM can be used to follow the accumulation of BaP in *Chlorella* cells. Our results suggest that BaP accumulates in lipid bodies and/or vacuoles of *Chlorella* for a long time (imaged up to 3 weeks) and that there is Förster resonance energy transfer (FRET) between BaP and photosystems of the cells. The localization of BaP in *Chlorella* cells could be visualized while avoiding the background fluorescence due to fluorescing molecules in the algal photosystems and the quenching of BaP fluorescence due to FRET. Our N&B analysis suggests that BaP predominantly exists as monomers rather than as aggregates inside the *Chlorella* cells.

■ EXPERIMENTAL DESIGN

Microalgal Culture. Axenic culture of the green unicellular microalga *Chlorella* sp., originally isolated from a soil sample and maintained in the Phycology Laboratory at the Centre for Environmental Risk Assessment and Remediation of the Environment (CERAR), University of South Australia, was used in this study. The culture was maintained in Bold's basal medium (BBM) as described earlier.²³ The culture was grown in 100 mL Erlenmeyer flasks containing 25 mL of BBM in an

orbital shaker set at 150 rpm under 3 × 36 W cool white fluorescent light (~100 μmol of photosynthetic photon flux density) at 24 ± 2 °C.²⁴

BaP Exposure Assay. Assays were conducted with exponentially growing culture of *Chlorella* sp. (3×10^4 cells mL⁻¹) in 25 mL of BBM placed in 100 mL sterile Erlenmeyer flasks. The cultures were examined in an Olympus BX41 epifluorescence microscope for the presence of any contaminating fluorescent materials or debris in the medium other than the autofluorescent microalgal cells. The culture was exposed to 100 μM BaP in culture medium added from a concentrated stock solution prepared in *N,N*-dimethylformamide (DMF) and incubated in an orbital shaker under constant illumination at 24 ± 2 °C as described above. An untreated culture incubated similarly to the treated culture served as a control. The samples were drawn for confocal microscopy analysis after 1, 5, 12, and 24 h of incubation with BaP.

Laser Confocal Microscopy. BaP and Nile red images were obtained with a Leica SPS inverted microscope using a 63×, 1.2 NA water immersion objective. BaP was prepared in DMF, resuspended in BBM, incubated with *Chlorella* cells, and used for imaging. BaP was excited with a 405 nm laser, and emission was set at 450–550 and 600–750 nm simultaneously in two channels. For Nile red staining, Nile red was prepared in DMF (~10 mM) and diluted into BBM to a final concentration of 100 μM. Nile red (100 μM) was incubated with *Chlorella* cells in 100 mL of BBM for 1 or 2 h and imaged in the confocal microscope. The fluorophore was excited using a 488 nm laser, and the emission window was set to 500–550 nm.

Fluorescence Lifetime Imaging Microscopy. FLIM was carried out using a Leica SPS microscope with a 405 nm pulsed laser at a frequency of 40 MHz. The emission window was set at 450–550 nm to collect the emission from BaP and 600–750 nm to collect the autofluorescence (predominantly Photosystems I and II) of algal cells. The image sizes were set at 256 × 256 pixels, and the signals were collected for 120 s. The FLIM data were analyzed using SimFCS software.²⁵

FLIM Data Analysis. Leica SpS time-correlated single-photon counting (TCSPC) lifetime image files (*.sdt) were opened in the SimFCS FLIM analysis module, and the phasor plot was generated using the Phasor Explorer page of SimFCS. The lifetime of fluorescein (4.1 ns) was used as a reference. The sample files were opened, and the different phasor plots for each file were generated and analyzed either to obtain lifetimes or to see quenching processes indicative of FRET.

The images were analyzed pixel by pixel using SimFCS software. The lifetime image has time delay information. The histogram of the time delays at each pixel is transformed into a phasor plot, which is like a vector. The phasor plot is a two-dimensional histogram where the values of the sine–cosine transforms are represented in a polar plot. Each pixel of the image has a point in the phasor plot. In a reciprocal manner, each point of the phasor plot can be mapped to a pixel of the image. Hence, each molecular species has a specific phasor; molecules can be identified by their position in the phasor plot.²⁶

Number and Brightness Analysis. N&B analysis was done according to the procedure of Dalal et al.²⁷ and Digman et al.²⁸ A time series of 100 frames with a resolution of 256 × 256 pixels, a pixel size of 49.7 nm, and a pixel dwell time of 8, 12, or 20 μs was collected using a Nikon C1-Z confocal imaging system (Nikon Eclipse TE2000-E with a 63×, 1.2 NA water immersion objective, Hanson Institute, Adelaide). The laser

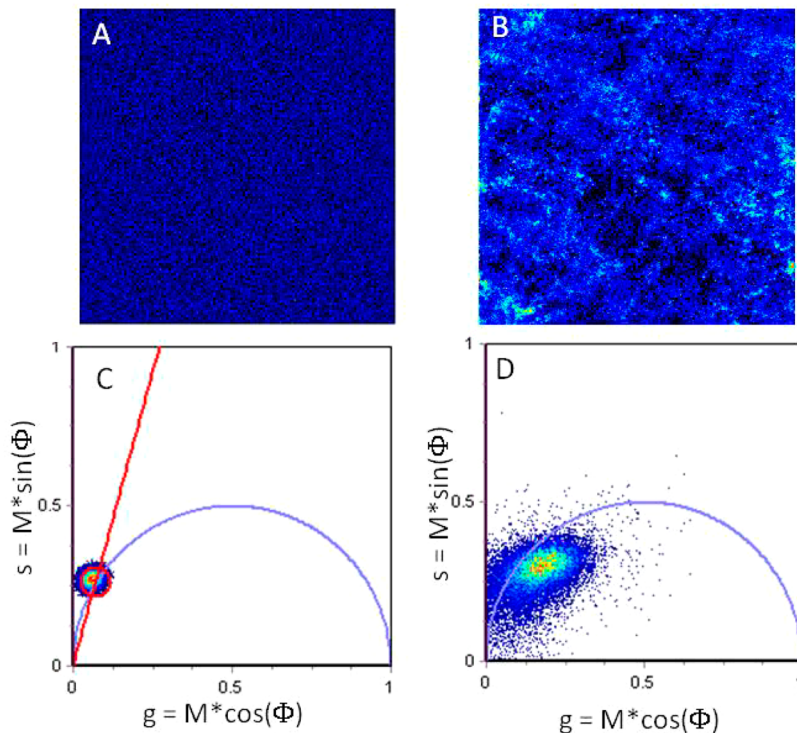


Figure 1. (A, B) Laser confocal microscopy images of BaP in (A) DMF and (B) BBM. (C, D) Phasor plots of lifetime images of BaP in (C) DMF and (D) BBM.

power was adjusted so as to prevent saturation of the detector. Background counts were collected with the laser off and the detectors on using the same gain and offset settings as used for collecting the time series. The *.ids files of the Nikon confocal microscope were converted to *.bin files and imported into SimFCS, and N&B analysis was performed.^{27,28} From the background files, the S factor and σ factor were estimated and used to analyze the data.

Sediment Chemical Analysis. Total organic carbon and inorganic carbon were measured using a total organic carbon analyzer (1010 TOC analyzer, OI Analytical, College Station, TX, USA). Phosphorus and potassium were measured from the aqua regia extract of sediments using inductively coupled plasma mass spectrometry (ICP-MS) (Agilent 7500 series, Agilent Technologies, Tokyo, Japan). Both pH and electrical conductivity were measured using the Smart CHEM-Lab laboratory analyzer (TPS Pty Ltd., Brisbane, Australia) and are reported in Table S2 in the Supporting Information.

BaP Uptake from Sediment by *Chlorella* sp. Sediments were collected from two locations in Barker's Wetlands, South Australia. Sediments were analyzed for the presence of BaP.²⁹ Sediments were spiked with BaP at two different concentrations (5 and 20 mg L^{-1}), and 20 g samples of spiked and unspiked sediments were weighed into sterile Petri dishes. Then the *Chlorella* cells were added to the sediments at a concentration of 5×10^5 cells (g of sediment) $^{-1}$ and incubated under continuous $3 \times 36\text{ W}$ cool white fluorescent light at $24 \pm 2^\circ\text{C}$. Samples were taken for fluorescence microscopy analysis after 1 , 5 , 12 , and 24 h of incubation. Cells that had BaP (blue fluorescence) and cells without BaP (red fluorescence) were counted separately. The effects of incubation time, BaP concentration, and sediment type and their interaction on the BaP uptake by *Chlorella* sp. were analyzed by three-way ANOVA using Minitab 16 statistical software.

RESULTS AND DISCUSSION

Lifetime Imaging of BaP. BaP dissolves in organic solvents because of its hydrophobic nature, and molecules are monodispersed in these solvents. However, to understand the uptake, accumulation, and degradation using biological systems, BaP must be suspended in an aqueous medium. BaP was dissolved in DMF and subsequently resuspended in BBM to the required concentration and used in this study. Hence, it is appropriate to image BaP in DMF and an aqueous medium and measure the lifetimes in these media. The image of BaP fluorescence in DMF is very uniform (Figure 1A) because the molecules are dissolved. However, at the resolution of our microscope it is not possible to see smaller molecular aggregates. The image of BaP in the aqueous medium shows aggregates of large size (Figure 1B). Comparing these two images and taking into account the hydrophobic nature of BaP, we concluded that BaP forms aggregates in BBM but is monodispersed in DMF. These observations were confirmed later, as discussed in Number and Brightness Analysis below.

FLIM of BaP was performed in DMF as well as in BBM. Fluorescein was used as a lifetime standard (4.1 ns) to reference the phasor plot (the phasor plot with the fluorescein lifetime is not shown). The BaP in DMF lifetime image was imported into SimFCS and plotted in the phasor plot (Figure 1C). The lifetime was found to be a relatively single exponential at 14 ns , as shown by the phasor cluster located very close to the universal circle (where all of the single-exponential decays are found).

For all of the solution and suspension samples, the fluorescence decay data were extracted from the images and analyzed using Globals for Spectroscopy software.²⁵ The fluorescein data were fit to a single component at 4.1 ns (Figure S1A in the Supporting Information); the deviations were very small. Similarly, BaP in DMF was analyzed by the

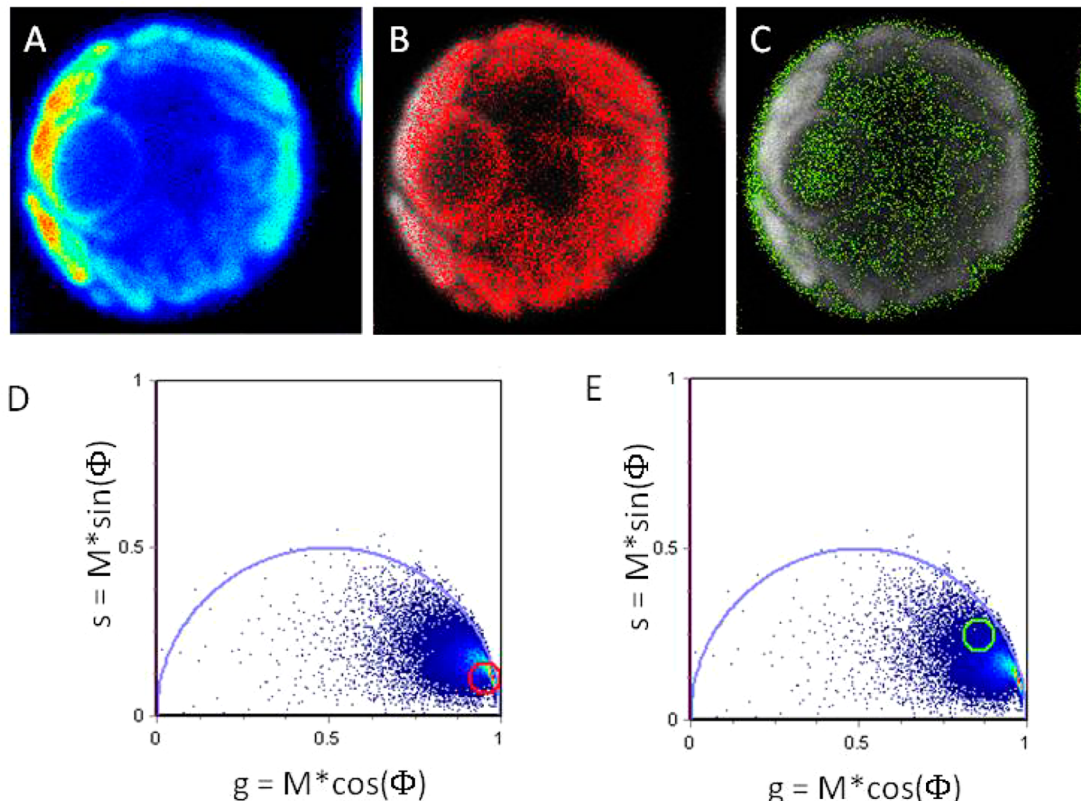


Figure 2. (A–C) Lifetime images of a *Chlorella* cell: (A) intensity image; (B) reciprocal plot selected by the cursor in the phasor plot in (D); (C) reciprocal plot selected by the cursor in the phasor plot in (E). (D, E) Phasor plots of fluorescence lifetimes of a *Chlorella* cell.

same algorithm (Figure S1B). There was a misfit of unknown origin at the very beginning of the data. However, the fit was much better when performed avoiding first part of the curve (Figure S1C). The recovered value of the lifetime using the least-squares analysis algorithm in Globals for Spectroscopy was 14.5 ns. One potential issue is that the intensity for this sample was very weak and there was a very large background. Also, the range that can be used for the B&H card was small, and there were artifacts at the beginning and the end of the time trace. Hence, this is a limitation with the instrumentation rather than experimental error.

The FLIM data of BaP in BBM in the phasor plot are scattered compared with those for BaP in DMF (Figure 1D), probably because the sample had very weak fluorescence and was aggregated. The average lifetime lies inside the semicircle with a broader distribution compared with that for BaP in DMF. This is expected because of the nature of BaP in the aqueous medium, which forms aggregates that are affected by self-quenching. Hence, the lifetime is shortened, shifting the phasor cluster toward smaller phase angles. The average lifetime for this sample was 7 ns, and the lifetimes were distributed between 12 and 4 ns. Our N&B analysis results correlate with this observation, as discussed below.

The lifetime of BaP in DMF was measured earlier by Iwata and co-workers³⁰ using the pulsed excitation method and further verified by them using the frequency domain method,³¹ and the lifetime was found to be 14.7 ns. This value is close to the lifetime that we obtained using lifetime imaging (14 ns). Furthermore, we obtained the lifetime of BaP in an aqueous medium (BBM). Vyas et al.³² used a TCSPC instrument to measure the lifetime of BaP in methanol and found the lifetime

to be 45 ns, which confirms an earlier report by Imasaka et al.³³ These measurements were carried out in cuvettes, and the data were fitted to obtain the lifetimes. The advantage with the phasor plot is that no fitting of the data is required.²⁸ Furthermore, the lifetime distribution in an image can be better visualized using the phasor plot. The broader lifetime distribution of BaP in BBM (Figure 1D) compared with BaP in DMF (Figure 1C) and the *Chlorella* sp. background lifetime (Figure 2D,E) are examples where the phasor plot gives a better understanding of the data, as there are no calculations or nonlinear fitting involved.²⁸ However, when the data do not show a distribution, as in the case of BaP in DMF, fitting routines could be used as well.

Lifetime Imaging of Auto fluorescence in the Micro-alga *Chlorella* sp. *Chlorella* sp. has several fluorescent molecules, among which chlorophyll a and b are the major ones. These molecules are part of Photosystems I and II. FLIM of *Chlorella* sp. was done as a control to understand the lifetime present in the background. As a result of energy transfer from Photosystem II to I and further down in the electron transport system, the lifetime of chlorophyll is very short. The lifetime measured from the phasor plot (Figure 2D,E) varied between 1.5 and 0.2 ns. The photosystems could not be distinguished, as the photosystem signals were collected in one channel. However, it is possible to separate regions of the cell with different lifetimes using the phasor plot. The majority of the pixels lifetimes were very short, around 200 ps in regions that can be associated with membranes, confirming that the background lifetime could arise from photosystems.

The lifetime image of a *Chlorella* cell is shown in Figure 2A. From this image, the phasor plot was generated (Figure 2D,E).

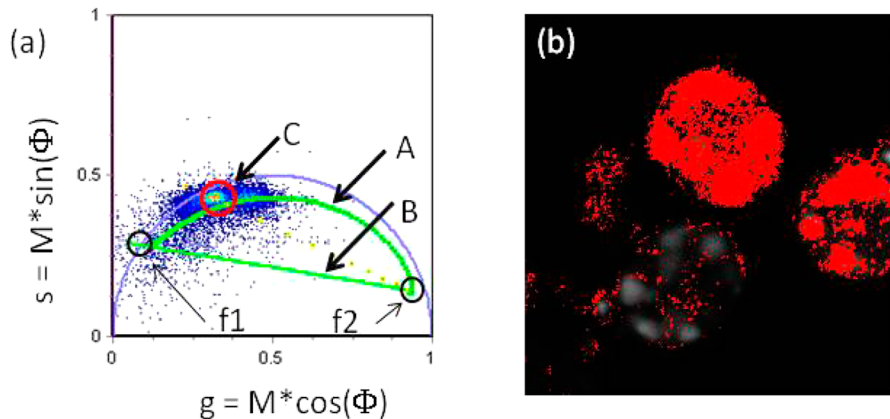


Figure 3. (a) Phasor plot showing the BaP lifetime distribution in *Chlorella* sp. The green line labeled as B represents linear combinations of the lifetimes of BaP and *Chlorella* background fluorescence, and the green curved trajectory labeled as A represents FRET between BaP and the photosystems. (b) Reciprocal selection from the phasor plot by the red cursor C in (a), showing the BaP fluorescence lifetime distribution in *Chlorella* sp.

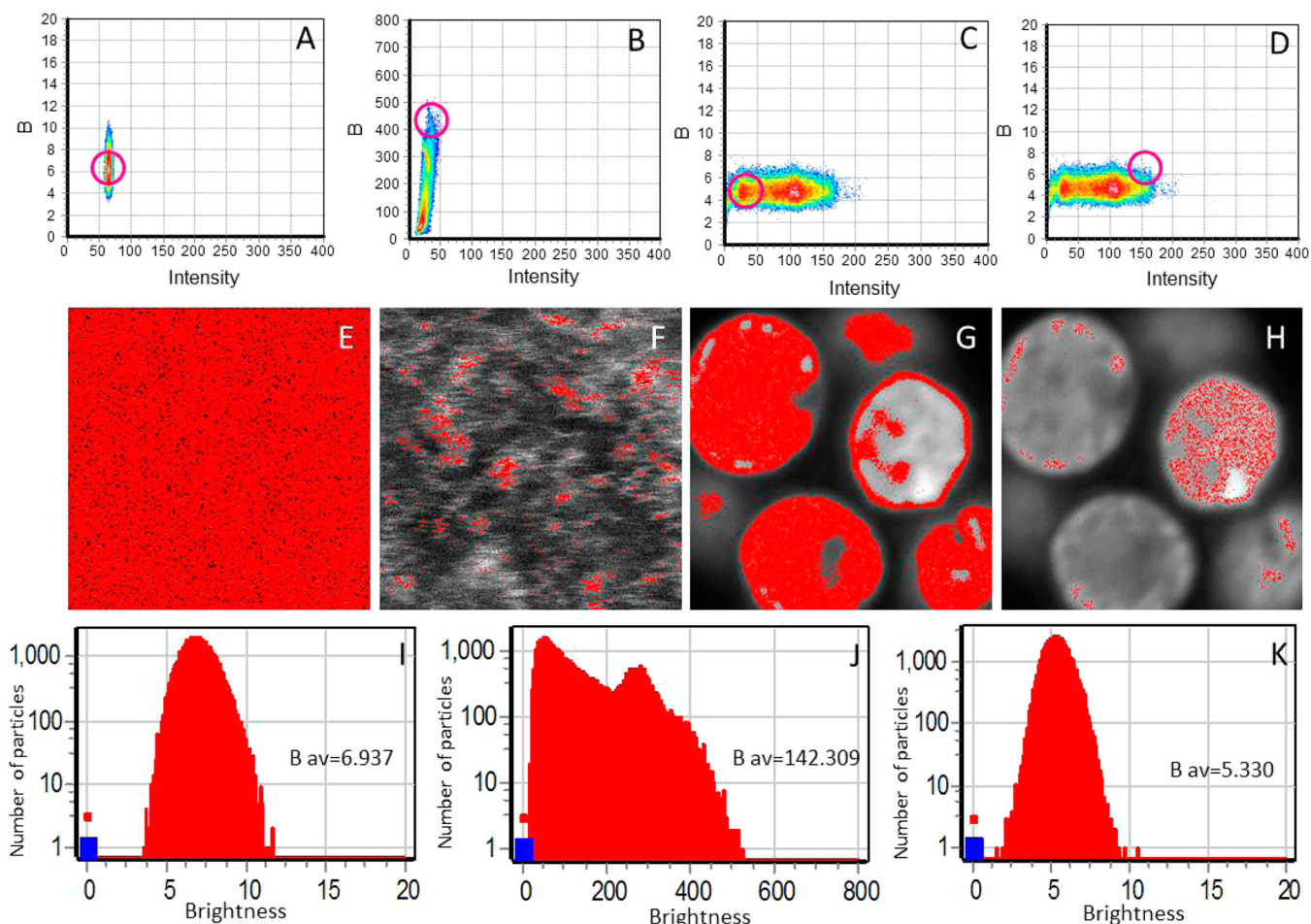


Figure 4. N&B analysis. (A–D) Maps of brightness vs fluorescence intensity for BaP in (A) DMF, (B) BBM, and (C, D) *Chlorella* sp. cells. (E) Image of BaP in DMF showing corresponding pixels selected by the cursor (red circle) in (A). (F) Image of BaP in BBM showing corresponding pixels selected by the cursor in (B), corresponding to high-brightness aggregates. (G) Image of BaP in *Chlorella* sp. cells showing corresponding pixels selected by the cursor in (C), corresponding to average-brightness particles. (H) Image of BaP in *Chlorella* sp. cells showing corresponding pixels selected by the cursor in (D), corresponding to high-brightness aggregates above average. (I–K) Histograms showing brightness distributions of BaP in (I) DMF, (J) BBM, and (K) *Chlorella* sp. cells.

In a reciprocal selection (from Figure 2D), a large cluster of phasor values was selected by the red cursor (red circle), and the pixels corresponding to that cluster are represented in red

in Figure 2B. Similarly, another cluster was selected in Figure 2E by the green cursor (green circle), and the corresponding pixels are painted in green in Figure 2C. Each lifetime selected

shows a different spatial pattern. However, it is difficult to interpret these results unequivocally as arising from a specific photosystem. Additional information could be obtained, for example, by using different quenchers to find out the distribution of certain fluorescent molecules in the photosystems.³⁴

Lifetime Imaging of BaP in *Chlorella* Cells. The phasor plot representation of the background lifetime of *Chlorella* cells, which is due to Photosystems I and II, is shown in Figure 2D,E. Similarly, the BaP lifetimes in DMF and BBM are plotted in phasor form in Figure 1C,D. When we combine these two components (BaP and background), the lifetime of BaP is reduced from 14 ns to about 8 ns (Figure 3a). We considered two possibilities: (1) that the reduction in the lifetime is due to the linear combination of the background lifetime and the BaP lifetime in the same pixel, and (2) that there could be quenching of the BaP fluorescence, making the BaP lifetime become shorter. It is a property of the phasor plot that the linear combination of lifetimes would fall somewhere on line B drawn in Figure 3a, depending on the contributions from the two components (f_1 and f_2).^{26,35} As the phasor plot shows, no phasor points are seen on that line. Hence, the BaP lifetime could be quenched by either Photosystem I or II, or both. If quenching of the donor BaP is due to FRET in which the photosystem acts as an acceptor, the phasor would fall anywhere in the quenching trajectory marked A in Figure 3a.²⁶ The red cursor in the phasor plot in Figure 3a selects the major phasor cluster, which has been reciprocally shown in red in Figure 3b.

However, the overall trend was that BaP was being quenched by the photosystems of *Chlorella* cells. The streaking curved nature of the phasor plot (Figure 3a) suggests varying quenching efficiencies of BaP fluorescence. Finally, another possibility is that BaP lifetime is shortened as a result of self-quenching.

Number and Brightness Analysis. The FLIM data suggest that there could be self-quenching of the BaP fluorescence and/or energy transfer from BaP to the photosystems. N&B analysis is an appropriate method to see whether there are aggregates of BaP in *Chlorella* cells. Time series (100 frames each) of BaP in DMF, BaP in BBM, and BaP in *Chlorella* cells were taken and analyzed. Figure 4A shows the N&B distribution of BaP in DMF. In DMF, molecules have an average brightness (B_{av}) of about 6.937, which after calibration corresponds to about 142 000 counts molecule⁻¹ s⁻¹. The brightness distribution is relatively narrow (Figure 4I). There is no evidence of dimers, which would have $B = 13$, or of larger aggregates. Figure 4A shows the distribution of the brightness and intensities selected.

In BBM, BaP forms aggregates. Figure 4B shows the distribution of intensity and brightness of the aggregates. A wide range of distribution of particles with varying brightness is shown in Figure 4J. In Figure 4B, the cursor (red circle) selects high-brightness pixels, and the corresponding bigger aggregates are highlighted in the image shown in Figure 4F. If we compare BaP in DMF and BaP in BBM, BaP exists as monodispersed molecules in DMF whereas it clearly aggregates in BBM.

In *Chlorella* cells, apart from background, there are varying intensity distributions (Figure 4C,D). A majority of pixels corresponding to the BaP fluorescence are selected by the red circle in Figure 4C and are mapped in red in Figure 4G. The average brightness is $B_{av} = 5.33$ (Figure 4K), which is slightly less than that for BaP in DMF (Figure 4I), indicating low

aggregation and some quenching. There are very few high-brightness particles ($B > 6$), which are selected by the red circle in Figure 4D and painted in red in Figure 4H. Figure 4G shows the reciprocal selection of pixels selected by the cursor (red circle) in Figure 4C, and similarly, Figure 4H shows the reciprocal selection by the cursor in Figure 4D. There are no larger aggregates seen as in the case of BaP in BBM.

Spectroscopic studies of BaP monomer, dimer, and trimer had been done by Fioretti et al.³⁶ BaP forms aggregates in aqueous media and is monodispersed in organic solvents. In a cell, as BaP prefers to partition into lipid droplets and the membrane portion, it is in a monomeric form. When BaP is taken up by a cell, it has to pass through the lipid bilayer, where it attaches as aggregates to the surface and then might dissociate. The aggregates might dissolve into the membrane and diffuse into cells. It is a general hypothesis that organic compounds pass passively through plant and animal cells.³⁷ However, experimental studies of individual organic pollutants and their interactions with different organisms are decisive if there is to be a clear depiction about the interaction properties of the pollutant with diverse organisms and cell types.

Accumulation of BaP in Lipid Bodies. *Chlorella* cells were incubated with BaP at a final concentration of 1, 40, or 100 μ M prepared in BBM and imaged. *Chlorella* cells incubated with BaP for 5 min and 48 h were imaged. There was no detectable difference in the accumulation patterns seen for the different incubation regimes of 5 min and 48 h using confocal microscopy. The cells showed accumulation of BaP in specific pockets (Figure 5B–E). These pockets could be lipid bodies and/or vacuoles considering the localization pattern of BaP. Thus, BaP could accumulate in these structures because of its hydrophobic nature.³⁸

Nile red, a lipid-specific dye,³⁹ was used to determine whether BaP accumulation occurs in lipid bodies of *Chlorella* cells. Nile red is excited at 488 nm and its emission maximum is at 525 nm, whereas BaP is excited at 405 nm and its emission is collected between 450 and 550 nm. As the emissions of these two dyes partially overlap, it is difficult to do simultaneous imaging and show colocalization. Hence, BaP and Nile red images were measured separately using different *Chlorella* cells, and the patterns are shown in Figure 5E,F, respectively. The Nile red pattern looks more diffuse with intense localization in lipid bodies. BaP localization shows an overall similar staining pattern with less diffuse staining. Compared to Nile red staining, BaP staining is more punctuated.

Study of BaP Uptake from Sediments by *Chlorella* sp. In order to determine the BaP uptake assay by microalgae, fluorescence microscopy analysis was carried out on *Chlorella* cells to detect the BaP uptake from sediments. There was not much difference in the BaP uptake by *Chlorella* sp. between the two sediments (denoted as S1 and S2), even though their nutrient contents differ greatly (Table S2 in the Supporting Information). BaP uptake could not be detected in the algae during the first and fifth hours of incubation, and all of the cells showed only background fluorescence. However, the number of cells with BaP fluorescence started to increase after 12 h of incubation (Figure 6). During the first few hours of incubation, the quantity of BaP taken up by microalgae may not be sufficient to detect using fluorescence microscopy. Moreover, no clear morphological differences between the *Chlorella* cells exposed to the BaP-spiked sediments and unspiked sediments were observed. Earlier, Wu et al.⁴⁰ observed morphological changes in *Aspergillus* fungus using fluorescence microscopy.

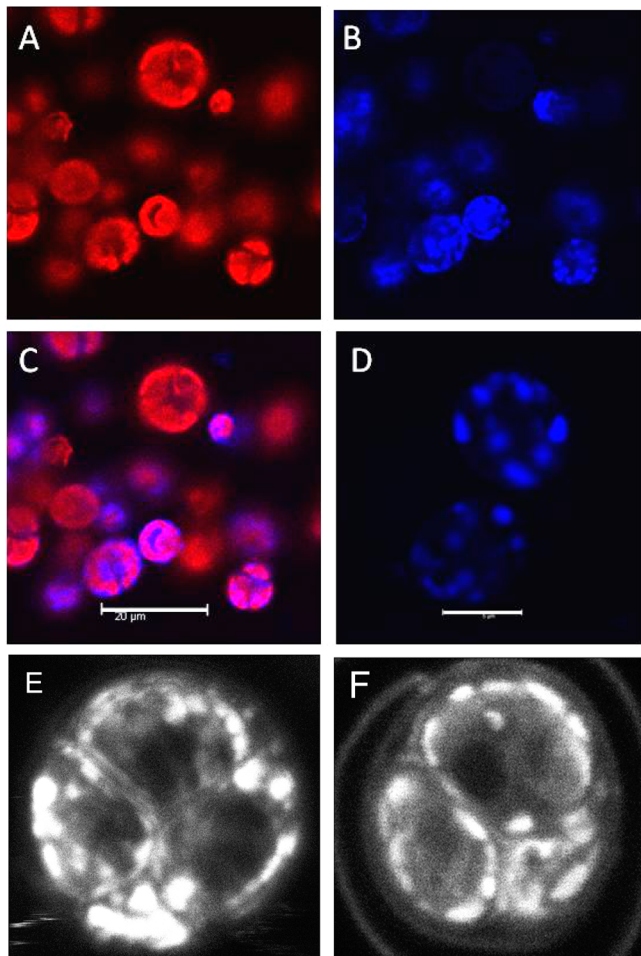


Figure 5. (A) Confocal microscopy image of *Chlorella* cells showing background photosystem fluorescence. (B) Confocal microscopy image showing BaP fluorescence in *Chlorella* cells. (C) Overlay of *Chlorella* sp. background fluorescence and BaP fluorescence (scale bar = 20 μ m). (D) Higher-magnification image showing fluorescence of BaP inside *Chlorella* sp. cells (scale bar = 5 μ m). (E) Confocal microscopy image of a *Chlorella* cell showing pectate staining of BaP fluorescence. (F) Confocal microscopy image of a *Chlorella* cell showing the lipid-specific fluorescent stain Nile red.

This shows the differential response between microalgae and fungi to BaP at the microscopic level.

Analysis by three-way ANOVA indicates that BaP concentration, incubation time, and sediment type all have significant effects ($p > 0.01$) on the BaP uptake by *Chlorella* sp. A significant influence of BaP concentration and incubation time was seen. A significant influence of incubation time and sediment type ($p > 0.01$) on BaP uptake was also observed. However, there was no significant interaction between BaP concentration and sediment type on the BaP uptake by *Chlorella* ($p > 0.01$).

Fluorescence Microscopy and BaP Uptake by Microalgae. FLIM, confocal microscopy, and N&B techniques can be used to study the uptake, accumulation, and aggregation of BaP in living cells. The limitations of imaging of BaP localization in *Chlorella* cells is that there is background fluorescence from photosystems and other molecules and there is FRET between BaP and other molecules in the cell. However, FLIM can be used to distinguish the background fluorescence from BaP fluorescence. N&B analysis can be used

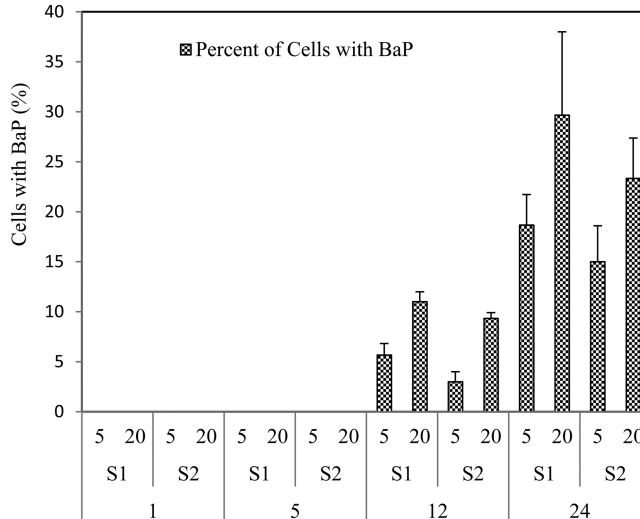


Figure 6. Fluorescence microscopy analysis of BaP uptake by *Chlorella* sp. in two different sediments (5 and 20 are BaP concentrations; S1 and S2 are sediment types; and 1, 5, 12, and 24 are incubation periods).

to determine whether BaP aggregates inside the cell. The advantages of using the FLIM–phasor and N&B analyses are that BaP fluorescence can be distinguished from the background fluorescence and aggregation of BaP molecules can be visualized inside the cells. In the case of *Chlorella* sp., BaP accumulates at high concentrations inside the cells, preferentially in lipid bodies. BaP forms aggregates of various sizes in an aqueous medium (BBM), whereas it exists as monomers or small aggregates inside the cell. This study lays the foundation for studying the interaction of microalgae and fluorescent xenobiotics such as BaP using confocal microscopy. Indeed, there is more potential for utilizing and refining this technique to study the interaction of fluorescent pollutants in other diverse microorganisms.

■ ASSOCIATED CONTENT

S Supporting Information

Fluorescence decay data and fitting for fluorescein and BaP and physicochemical properties of the sediments used in this study. This material is available free of charge via the Internet at <http://pubs.acs.org>.

■ AUTHOR INFORMATION

Corresponding Author

*E-mail: Kannan.krishnan@unisa.edu.au; tel: +61 (0) 8 8302 5068; fax: +61 8 8302 3057.

Notes

The authors declare no competing financial interest.

■ ACKNOWLEDGMENTS

The authors thank Ms. Lyn Waterhouse (Adelaide Microscopy, The University of Adelaide), Dr. Jennifer Clarke (School of Medicine, Flinders University), and Dr. Ghafar Sarvestani (Hanson Institute, Adelaide, South Australia) for their support with confocal microscopy. S.R.S. acknowledges UniSA for providing a UPS Scholarship and CRC CARE for a Ph.D. scholarship. This work was supported in part by NIH (Grants P41 GM GM103540 and P50 GM076516 grants to E.G.).

■ REFERENCES

- (1) Ravindra, K.; Sokhi, R.; Van Grieken, R. Atmospheric polycyclic aromatic hydrocarbons: Source attribution, emission factors and regulation. *Atmos. Environ.* **2008**, *42* (13), 2895–2921.
- (2) Gelboin, H. Benzo[a]pyrene metabolism, activation and carcinogenesis: Role and regulation of mixed-function oxidases and related enzymes. *Physiol. Rev.* **1980**, *60* (4), 1107–1166.
- (3) Janikowska, G.; Wardas, W. Bioconcentration of benzo[a]pyrene in *Chlorella* BB cells. *Pol. J. Environ. Stud.* **2002**, *11* (4), 345–348.
- (4) Canova, S.; Degan, P.; Peters, L. D.; Livingstone, D. R.; Voltan, R.; Venier, P. Tissue dose, DNA adducts, oxidative DNA damage and CYP1A-immunopositive proteins in mussels exposed to waterborne benzo[a]pyrene. *Mutat. Res.* **1998**, *399* (1), 17–30.
- (5) Bock, F. G.; Smith, D. H.; Dao, T. L. Deposition of benzo[a]pyrene in mouse fat after oral administration. *Cancer Res.* **1964**, *24* (2Part 1), 280–285.
- (6) Wainright, S.; Weinstein, M.; Able, K.; Currin, C. Relative importance of benthic microalgae, phytoplankton and the detritus of smooth cordgrass *Spartina alterniflora* and the common reed *Phragmites australis* to brackish-marsh food webs. *Mar. Ecol.: Prog. Ser.* **2000**, *200*, 77–91.
- (7) Okay, O. S.; Donkin, P.; Peters, L. D.; Livingstone, D. R. The role of algae (*Isochrysis galbana*) enrichment on the bioaccumulation of benzo[a]pyrene and its effects on the blue mussel *Mytilus edulis*. *Environ. Pollut.* **2000**, *110* (1), 103–113.
- (8) Semple, K.; Cain, R.; Schmidt, S. Biodegradation of aromatic compounds by microalgae. *FEMS Microbiol. Lett.* **1999**, *170* (2), 291–300.
- (9) Rosas, I.; Velasco, A.; Belmont, R.; Báez, A.; Martínez, A. The algal community as an indicator of the trophic status of Lake Patzcuaro, Mexico. *Environ. Pollut.* **1993**, *80* (3), 255–264.
- (10) Lindquist, B.; Warshawsky, D. Identification of the 11,12-dihydro-11,12-dihydroxybenzo[a]pyrene as a major metabolite produced by the green alga, *Selenastrum capricornutum*. *Biochem. Biophys. Res. Commun.* **1985**, *130* (1), 71–75.
- (11) Warshawsky, D.; Radike, M.; Jayasimhulu, K.; Cody, T. Metabolism of benzo[a]pyrene by a dioxygenase enzyme system of the freshwater green alga *Selenastrum capricornutum*. *Biochem. Biophys. Res. Commun.* **1988**, *152* (2), 540–544.
- (12) Warshawsky, D.; Keenan, T. H.; Reilman, R.; Cody, T. E.; Radike, M. J. Conjugation of benzo[a]pyrene metabolites by freshwater green alga *Selenastrum capricornutum*. *Chem.-Biol. Interact.* **1990**, *74* (1–2), 93–105.
- (13) Nebert, D. W.; Roe, A. L.; Dieter, M. Z.; Solis, W. A.; Yang, Y.; Dalton, T. P. Role of the aromatic hydrocarbon receptor and [Ah] gene battery in the oxidative stress response, cell cycle control, and apoptosis. *Biochem. Pharmacol.* **2000**, *59* (1), 65–85.
- (14) Kim, J. Y.; Chung, J.-Y.; Park, J.-E.; Lee, S. G.; Kim, Y.-J.; Cha, M.-S.; Han, M. S.; Lee, H.-J.; Yoo, Y. H.; Kim, J.-M. Benzo[a]pyrene induces apoptosis in RL95-2 human endometrial cancer cells by cytochrome P450 1A1 activation. *Endocrinology* **2007**, *148* (10), 5112–5122.
- (15) Shi, S.; Yoon, D. Y.; Hodge-Bell, K. C.; Bebenek, I. G.; Whitekus, M. J.; Zhang, R.; Cochran, A. J.; Huerta-Yepes, S.; Yim, S.-H.; Gonzalez, F. J.; Jaiswal, A. K.; Hankinson, O. The aryl hydrocarbon receptor nuclear translocator (Arnt) is required for tumor initiation by benzo[a]pyrene. *Carcinogenesis* **2009**, *30* (11), 1957–1961.
- (16) Hsu, G. W.; Huang, X.; Luneva, N. P.; Geacintov, N. E.; Beese, L. S. Structure of a high fidelity DNA polymerase bound to a benzo[a]pyrene adduct that blocks replication. *J. Biol. Chem.* **2005**, *280* (5), 3764–3770.
- (17) Solhaug, A.; Refsnes, M.; Låg, M.; Schwarze, P. E.; Husøy, T.; Holme, J. A. Polycyclic aromatic hydrocarbons induce both apoptotic and anti-apoptotic signals in Hepa1c1c7 cells. *Carcinogenesis* **2004**, *25* (5), 809–819.
- (18) Plant, A. L.; Benson, D. M.; Smith, L. C. Cellular uptake and intracellular localization of benzo[a]pyrene by digital fluorescence imaging microscopy. *J. Cell Biol.* **1985**, *100* (4), 1295–1308.
- (19) Hornung, M. W.; Cook, P. M.; Fitzsimmons, P. N.; Kuehl, D. W.; Nichols, J. W. Tissue distribution and metabolism of benzo[a]pyrene in embryonic and larval medaka (*Oryzias latipes*). *Toxicol. Sci.* **2007**, *100* (2), 393–405.
- (20) Walker, R. F.; Ishikawa, K.; Kumagai, M. Fluorescence-assisted image analysis of freshwater microalgae. *J. Microbiol. Methods* **2002**, *51* (2), 149–162.
- (21) Holub, O.; Seufferheld, M. J.; Gohlke, C.; Heiss, G. J.; Clegg, R. M. Fluorescence lifetime imaging microscopy of *Chlamydomonas reinhardtii*: Non-photochemical quenching mutants and the effect of photosynthetic inhibitors on the slow chlorophyll fluorescence transient. *J. Microsc.* **2007**, *226* (2), 90–120.
- (22) Holub, O.; Seufferheld, M. J.; Gohlke, C.; Govindjee; Clegg, R. M. Fluorescence lifetime imaging (FLI) in real-time—A new technique in photosynthesis research. *Photosynthetica* **2000**, *38* (4), 581–599.
- (23) Megharaj, M.; Venkateswarlu, K.; Rao, A. Growth response of four species of soil algae to monocrotaphos and quinalphos. *Environ. Pollut.* **1986**, *42* (1), 15–22.
- (24) Megharaj, M.; Singleton, I.; McClure, N. C.; Naidu, R. Influence of petroleum hydrocarbon contamination on microalgae and microbial activities in a long-term contaminated soil. *Arch. Environ. Contam. Toxicol.* **2000**, *38* (4), 439–445.
- (25) Laboratory for Fluorescence Dynamics Website. <http://www.lfd.uci.edu/globals> (accessed July 17, 2013).
- (26) Digman, M. A.; Caiolfa, V. R.; Zamai, M.; Gratton, E. The phasor approach to fluorescence lifetime imaging analysis. *Biophys. J.* **2008**, *94* (2), L14–L16.
- (27) Dalal, R. B.; Digman, M. A.; Horwitz, A. F.; Vetri, V.; Gratton, E. Determination of particle number and brightness using a laser scanning confocal microscope operating in the analog mode. *Microsc. Res. Technol.* **2008**, *71* (1), 69–81.
- (28) Digman, M. A.; Dalal, R.; Horwitz, A. F.; Gratton, E. Mapping the number of molecules and brightness in the laser scanning microscope. *Biophys. J.* **2008**, *94* (6), 2320–2332.
- (29) Thavamani, P.; Megharaj, M.; Krishnamurti, G. S. R.; McFarland, R.; Naidu, R. Finger printing of mixed contaminants from former manufactured gas plant (MGP) site soils: Implications to bioremediation. *Environ. Int.* **2011**, *37* (1), 184–189.
- (30) Iwata, T.; Tanaka, T.; Komatsu, T.; Araki, T. An externally controlled, nanosecond-pulsed, Xe lamp using a high voltage semiconductor switch. *Rev. Sci. Instrum.* **2000**, *71* (11), 4045–4049.
- (31) Iwata, T.; Hori, A.; Kamada, T. Photon-counting phase-modulation fluorometer. *Opt. Rev.* **2001**, *8* (5), 326–330.
- (32) Vyas, S.; Onchoke, K. K.; Rajesh, C. S.; Hadad, C. M.; Dutta, P. K. Optical spectroscopic studies of mononitrated benzo[a]pyrenes. *J. Phys. Chem. A* **2009**, *113* (45), 12558–12565.
- (33) Imasaka, T.; Kawabata, Y.; Ishibashi, N. Subnanosecond time correlated photon counting spectroscopy with atmospheric pressure nitrogen laser pumped dye lasers. *Rev. Sci. Instrum.* **1981**, *52* (10), 1473–1477.
- (34) Gilmore, A. M.; Hazlett, T. L.; Govindjee. Xanthophyll cycle-dependent quenching of photosystem II chlorophyll a fluorescence: Formation of a quenching complex with a short fluorescence lifetime. *Proc. Natl. Acad. Sci. U.S.A.* **1995**, *92* (6), 2273–2277.
- (35) Colyer, R. A.; Lee, C.; Gratton, E. A novel fluorescence lifetime imaging system that optimizes photon efficiency. *Microsc. Res. Technol.* **2008**, *71* (3), 201–213.
- (36) Fioretti, S. E.; Binning, R. C., Jr.; Bacelo, D. E. Effects of cluster formation on spectra of benzo[a]pyrene and benzo[e]pyrene. *Chem. Phys. Lett.* **2008**, *454* (4–6), 269–273.
- (37) Della Greca, M.; Pinto, G.; Pistillo, P.; Pollio, A.; Previtera, L.; Temussi, F. Biotransformation of ethinylestradiol by microalgae. *Chemosphere* **2008**, *70* (11), 2047–2053.
- (38) Vasiluk, L.; Pinto, L. J.; Tsang, W. S.; Gobas, F. A. P. C.; Eickhoff, C.; Moore, M. M. The uptake and metabolism of benzo[a]pyrene from a sample food substrate in an in vitro model of digestion. *Food Chem. Toxicol.* **2008**, *46* (2), 610–618.

- (39) Greenspan, P.; Mayer, E. P.; Fowler, S. D. Nile red: A selective fluorescent stain for intracellular lipid droplets. *J. Cell Biol.* **1985**, *100* (3), 965–973.
- (40) Wu, Y.-R.; He, T.-T.; Lun, J.-S.; Maskooui, K.; Huang, T.-W.; Hu, Z. Removal of benzo[*a*]pyrene by a fungus *Aspergillus* sp. BAP14. *World J. Microbiol. Biotechnol.* **2009**, *25* (8), 1395–1401.